© 2016. Published by The Company of Biologists Ltd | Development (2016) 143, 4755 doi:10.1242/dev.146209

CORRECTION

Correction: Mice humanised for the EGF receptor display hypomorphic phenotypes in skin, bone and heart

Maria Sibilia, Bettina Wagner, Astrid Hoebertz, Candace Elliott, Silvia Marino, Wolfram Jochum and Erwin F. Wagner

There was an error published in Development **130**, 4515-4525.

In Fig. 6, owing to an error in figure assembly during preparation of the proofs, the incorrect image (a duplication of panel D) was displayed in panel G. The corrected figure appears below.

We apologise to the authors and readers for this mistake.

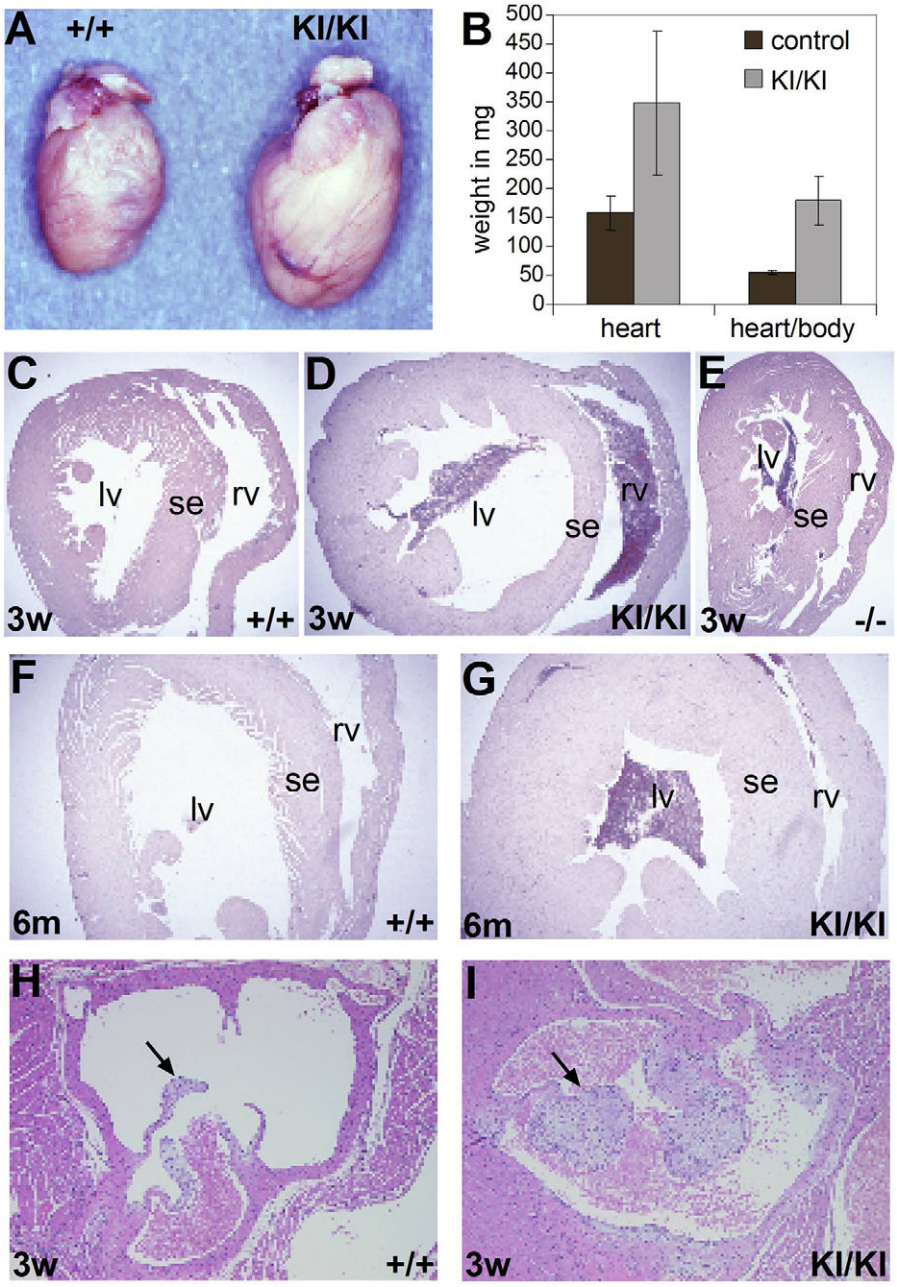

Mice humanised for the EGF receptor display hypomorphic phenotypes in skin, bone and heart

Maria Sibilia[1,2,*], Bettina Wagner[1], Astrid Hoebertz[2], Candace Elliott[2,†], Silvia Marino[3,‡], Wolfram Jochum[2,‡] and Erwin F. Wagner[2]

[1]Department of Dermatology and Biomolecular Therapeutics (BMT), University of Vienna, Medical School, Brunnerstr. 59, A-1235 Vienna, Austria
[2]Research Institute of Molecular Pathology (IMP), Dr Bohr-Gasse 7, A-1030 Vienna, Austria
[3]Division of Molecular Genetics and Centre of Biomedical Genetics, The Netherlands Cancer Institute, 1066CX Amsterdam, The Netherlands

*Author for correspondence (e-mail: maria.sibilia@univie.ac.at)
†Present address: School of Botany, University of Melbourne, Victoria 3010, Australia
‡Present address: Institute of Clinical Pathology, University Hospital Zurich, Schmelzbergstrasse 12, CH-8091 Zurich, Switzerland

Accepted 12 June 2003

Development 130, 4515-4525

doi:10.1242/dev.00664

Summary

Mice lacking the epidermal growth factor receptor (EGFR) develop epithelial defects and a neurodegenerative disease and die within the first month of birth. By employing a conditional knock-in approach using the human *EGFR* cDNA mice humanised for EGFR (*hEGFR$^{KI/KI}$*) were generated. Homozygous *hEGFR$^{KI/KI}$* mice are viable and live up to six months. However, these mice are growth retarded and show skin and hair defects similar to *Egfr$^{-/-}$* mutants. Interestingly, the neurodegeneration is fully rescued in *hEGFR$^{KI/KI}$* mice, however, they develop a severe heart hypertrophy with semilunar valve abnormalities. Moreover, *hEGFR$^{KI/KI}$* mice display accelerated chondrocyte and osteoblast differentiation, a phenotype that is also present in *Egfr$^{-/-}$* mice and has not been previously described. The severity of the phenotypes correlates with the expression levels of the *hEGFR^{KI}* allele, which is not efficiently expressed in epithelial and bone cells, but is expressed at similar and even higher levels as the endogenous *Egfr* in brain and heart. These results demonstrate that mice humanised for EGFR display tissue-specific hypomorphic phenotypes and describe a novel function for EGFR in bone development.

Key words: Bone, Hair growth, Heart hypertrophy, Humanised *EGFR* knock-in mice, Skin

Introduction

The epidermal growth factor receptor (EGFR/Erbb1) belongs to a family of structurally related tyrosine kinase receptors, including Erbb2/neu, Erbb3 and Erbb4, which upon ligand binding can form homo- and heterodimers (Olayioye et al., 2000; Schlessinger, 2000; Yarden and Sliwkowski, 2001). Several growth factors such as epidermal growth factor (EGF), transforming growth factor α (TGFα), amphiregulin, heparin-binding EGF (HB-EGF), β-cellulin and epiregulin can bind the EGFR and induce receptor dimerisation. Subsequent activation of the intrinsic tyrosine kinase induces complex downstream signalling pathways, which can instruct cells either to proliferate, differentiate and/or survive. Little is known about how these cellular responses are regulated in different cell types in vivo (Olayioye et al., 2000; Yarden and Sliwkowski, 2001).

Most of the current knowledge about the function of the EGFR and its family members during normal development derives from the analysis of mutant mice. Mice lacking *Erbb2*, *Erbb3* and *Erbb4* die at midgestation, because of cardiac dysfunction associated with lack of ventricular trabeculation, and display abnormal development of the peripheral nervous system (Gassmann et al., 1995; Lee et al., 1995; Riethmacher et al., 1997). Inactivation of the *Egfr* in mice reveals that mutant mice die at midgestation (129/Sv), birth (C57BL/6) or can live up to postnatal day 20 (MF1, C3H and CD1) depending on their genetic background. They exhibit epithelial and neural phenotypes as well as craniofacial malformations (Miettinen et al., 1995; Miettinen et al., 1999; Sibilia and Wagner, 1995; Threadgill et al., 1995). Death in utero results from a placental defect, as the embryonic lethality can be rescued by generating aggregation chimeras between *Egfr$^{-/-}$* and tetraploid wild-type embryos, the latter contributing exclusively to extra-embryonic tissues (Sibilia et al., 1998). Independent of the genetic background, surviving *Egfr$^{-/-}$* mice develop a progressive neurodegeneration in the olfactory bulbs and frontal cortex, which is characterised by massive apoptotic cell death affecting both neurones and astrocytes (Kornblum et al., 1998; Sibilia et al., 1998). Ectopic neurones are always detected in the white matter of the hippocampus, suggesting that EGFR signalling might be important for neuronal migration (Sibilia et al., 1998). The lack of EGFR does not seem to affect the self-renewing potential of neural progenitors in response to FGF (Tropepe et al., 1999). However, EGFR is crucial for astrocyte development, as cerebral cortices from *Egfr$^{-/-}$* mice contain lower numbers of astrocytes, which

display a severe proliferation defect in vitro (Kornblum et al., 1998; Sibilia et al., 1998). Therefore, the EGFR is most probably required for the proliferation/differentiation of astrocytes and for preserving brain integrity after birth.

In addition to the neural defects, *Egfr*$^{-/-}$ mice also display several abnormalities in epithelial tissues. They are born with open eyes and show impaired epidermal as well as hair follicle differentiation and fail to develop a hairy coat most likely because EGFR signalling is necessary for maintenance of hair follicle integrity (Miettinen et al., 1995; Sibilia and Wagner, 1995; Threadgill et al., 1995). However, *Egfr*$^{-/-}$ mice do not survive beyond the termination of the first hair cycle and, therefore, a careful analysis of EGFR function during skin and hair follicle development could not be performed. Grafting experiments of *Egfr*$^{-/-}$ skin explants on athymic nude mice suggest that *Egfr*$^{-/-}$ follicles cannot proceed from the anagen to telogen phase of the hair cycle (Hansen et al., 1997). These alterations eventually lead to necrosis and disappearance of the follicles, accompanied by strong infiltration of the skin with inflammatory cells (Hansen et al., 1997). A similar but more severe skin and hair phenotype could be detected in transgenic mice expressing a dominant negative (DN) *Egfr* (CD533) from the keratin 5 (K5) promoter (Murillas et al., 1995). However, in these mice it could not be excluded that other Erbb receptors were also inhibited by the DN EGFR, thereby exacerbating the skin defects. Milder phenotypes characterised by a 'wavy' coat and curly whiskers are observed in mice deficient for the gene encoding TGFα and in mice homozygous for the hypomorphic *Egfr* allele waved 2 (*wa2*), which carry a point mutation in the kinase domain of the EGFR resulting in a drastically reduced kinase activity (Fowler et al., 1995; Luetteke et al., 1994; Luetteke et al., 1993; Mann et al., 1993).

Numerous studies have documented alterations in EGFR signalling pathways in the development of human neoplasms (Olayioye et al., 2000; Yarden, 2001). Amplifications, rearrangements and overexpression of the *Egfr* gene have been shown to occur at high frequency in human squamous cell carcinomas and glioblastomas (Olayioye et al., 2000; Yarden, 2001). The first in vivo evidence for a direct involvement of the EGFR in epithelial tumour development stems from the analysis of transgenic mice expressing an activated form of the Ras activator son of sevenless (*Sos*) from the K5 promoter (Sibilia et al., 2000). All *K5-Sos* transgenic mice develop skin tumours only in the presence of a functional EGFR. *K5-Sos* transgenic skin papillomas in a EGFR mutant background show increased apoptosis and are more differentiated indicating that signalling through the EGFR enhances the survival and inhibits differentiation of epidermal cells (Sibilia et al., 2000). This is supported by the fact that *Egfr* is most strongly expressed in the proliferating compartments of the basal layer of the epidermis and in the outer root sheath of the hair follicles, and the number of receptors decreases as keratinocytes enter the pathway of terminal differentiation and migrate to the suprabasal layers of the epidermis (Peus et al., 1997; Sibilia and Wagner, 1995; Stoll et al., 2001).

The function of the EGFR in adult mice could not be addressed because of the early postnatal lethality of EGFR-deficient mice. Here, we employed a knock-in strategy to generate mice in which the endogenous mouse *Egfr* is replaced by a human *EGFR* cDNA that is flanked by loxP sites (*hEGFR*^{KI} allele). This approach enables the generation of humanised EGFR mice (*hEGFR*$^{KI/KI}$ mice) to study the functional homologies between the mouse and human EGFR in a conditional way. In addition, the phenotypic consequences of knocking-in well characterised human EGFR mutants can also be addressed. Homozygous *hEGFR*$^{KI/KI}$ mice are growth retarded but can survive for up to 6 months after birth. However, they display skin and hair growth defects similar to surviving *Egfr*$^{-/-}$ mice. Interestingly, the neurodegeneration is fully rescued, although *hEGFR*$^{KI/KI}$ mice develop a severe heart hypertrophy with abnormalities in semilunar valve development. Accelerated chondrocyte and osteoblast differentiation are detected in both *hEGFR*$^{KI/KI}$ and *Egfr*$^{-/-}$ mice, suggesting that EGFR signalling negatively regulates bone cell differentiation. The severity of the phenotypes correlates with the expression levels of the *hEGFR*^{KI} allele in various tissues. In bone cells and epithelial tissues the expression of the *hEGFR*^{KI} allele is severely reduced, whereas the *hEGFR*^{KI} allele is expressed at similar levels as the endogenous mouse gene in the brain thereby rescuing the neurodegeneration. Moreover, higher levels of expression of the *hEGFR*^{KI} allele are detected in the heart and are likely responsible for the development of the heart hypertrophy. These results demonstrate that mice humanised for EGFR display tissue-specific hypomorphic phenotypes thereby uncovering novel functions of the EGFR in bone and heart development.

Materials and methods

Generation of targeting construct and *hEGFR*$^{KI/KI}$ mice

To generate the EGFR knock-in vector the pGNA-based knock-out vector described previously (Sibilia and Wagner, 1995) was modified as follows. The *lacZ* gene was removed and replaced by a multiple cloning site. A loxP-flanked human *EGFR* (*hEGFR*) cDNA was inserted into the multiple cloning site and the vector was linearised with *Xba*I before electroporation into feeder-dependent GS-1 ES cells. Selection and screening of ES cell colonies by PCR and Southern blot analysis was performed as previously described (Sibilia and Wagner, 1995). Two correctly targeted ES cell clones were injected into C57BL/6 blastocysts and germline male chimeric mice were obtained with both clones. Chimeras were mated to 129/Sv and/or C57BL/6 females to obtain *hEGFR*$^{Ki/+}$ mice of inbred 129/Sv and mixed 129/Sv × C57BL/6 background, which were used for further breeding and generation of *hEGFR*$^{KI/KI}$ mice. Genotyping of the mice was performed by PCR as previously described (Sibilia and Wagner, 1995).

Histology

Mice were sacrificed and tissues were fixed in 4% PBS-buffered formaldehyde and embedded in paraffin wax. Sections (5 μm) were cut and stained with Haematoxylin and Eosin (Sigma Immunochemicals) according to standard procedures. Immunohistochemical staining for Ki67 (Novocastra, NCL-Ki67p, 1:1000) was performed using the ABC staining kit (Vector Laboratories) according to the manufacturer's recommendations. For histomorphometric analysis, Haematoxylin and Eosin stained cross-sections of hearts from 2.5- to 3.5-month-old *hEGFR*$^{KI/KI}$ mice (n=4) and age-matched controls (n=4) were evaluated using an Axioskop microscope (Carl Zeiss, Oberkochen, Germany) with integrated morphometric device at 400× magnification. The size of perpendicularly cut cardiomyocytes was determined in the subendocardial layers of the left ventricle.

RNAse protection assay

Total RNA was extracted and purified from various organs using

TRIzol reagents (Gibco) and subjected to RNAse protection analysis as previously described (Fleischmann et al., 2000). For the generation of the EGFR riboprobe, the region encompassing the 3′ end of the *Egfr* mouse promoter, the loxP site and the 5′ end of the *hEGFR* cDNA were cloned into SP64 plasmid, linearised and transcribed in vitro using the in vitro translation Kit from Stratagene.

Western blot analysis and in vitro EGFR autophosphorylation assay

Protein lysates were prepared from various tissues, cleared by centrifugation and either processed for western blot analysis or subjected to immunoprecipitation employing the rabbit anti EGFR antibody #1001 (Santa Cruz) as previously described (Sibilia et al., 2000; Sibilia and Wagner, 1995). Immunoprecipitated EGFR complexes were resuspended in 20 μl HNTG (20 mM HEPES pH 7.5, 150 mM NaCl, 0.1% Triton X-100, 10% Glycerol) containing 0.4 μl γ^{32}PdATP (10 μC/μl, Amersham) and incubated for 15 minutes on ice. Kinase reactions were stopped and protein complexes separated on 10% SDS-PAGE. Gels were dried at 80°C under vacuum and exposed to X-ray films (Amersham). Western blot analysis was performed with the anti EGFR antibody #06-129 (Upstate, 1:1000).

Astrocyte cultures

Primary astrocyte cultures were prepared from brains of newborn mice as previously described (Sibilia et al., 1998). Cells were plated in DMEM/F12 (1:1, GIBCO) culture medium containing 10% foetal calf serum (PAA) and after reaching confluency passaged at a 1:3 split ratio. Before replating, viable cell numbers were determined using a Neubauer-type haemocytometer with Trypan Blue staining (Sigma). The primary cultures consisted of >95% GFAP- (Sigma) positive astrocytes.

Osteoblast culture

Primary osteoblasts were isolated from calvariae of neonatal *hEGFR*$^{KI/KI}$, *Egfr*$^{-/-}$ and wild-type mice. Calvariae were sequentially digested for 10 minutes at 37°C in α-MEM (GIBCO) containing 0.1% collagenase and 0.2% dispase (Roche). Cells isolated in fractions 2-5 were combined as an osteoblastic cell population, expanded twice for 2-3 days in α-MEM with 10% foetal calf serum (PAA), and either replated in α-MEM for proliferation assays (10^5 cells/well in a 6-well plate), or in α-MEM supplemented with 5 mM β-glycerolphosphate and 100 μg/ml ascorbic acid (Sigma) (10^5 cells/well in a 24-well plate) for bone nodule assays.

Results

Generation of *hEGFR*$^{KI/KI}$ mice

To generate mice humanised for EGFR a gene-targeting vector was constructed, which after homologous recombination replaces parts of the first exon of the mouse *Egfr* gene with the loxP-flanked human *EGFR* cDNA (referred to as *hEGFR*^{KI} allele, Fig. 1A). This vector is a modified version of the one previously employed to generate *Egfr* knockout (*Egfr*$^{-/-}$) mice (Sibilia and Wagner, 1995). The construct was electroporated into ES cells and correctly targeted clones were identified by PCR and Southern blot analysis (data not shown). Two independent ES clones were injected into blastocysts and both formed germline chimeras. Heterozygous *hEGFR*$^{KI/+}$ mice of inbred 129/Sv or mixed 129/Sv×C57BL/6 background were intercrossed to generate *hEGFR*$^{KI/KI}$ mice, which were identified by PCR analysis

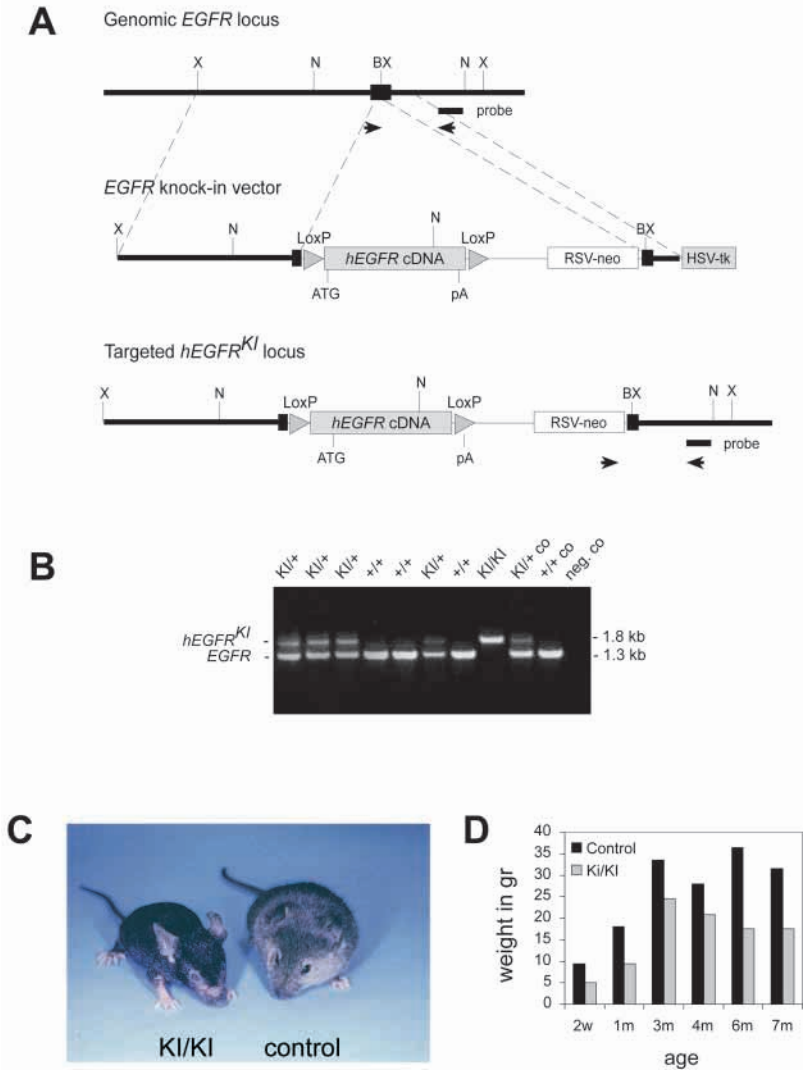

Fig. 1. Generation of *hEGFR*$^{KI/KI}$ mice. (A) Schematic representation of the targeting strategy employed to insert a floxed human *EGFR* cDNA (*hEGFR*) into the mouse *Egfr* locus. The full-length *hEGFR* expression cassette (grey box) contains its own ATG and polyA (pA) site and is flanked by loxP sites (grey triangles). After homologous recombination, the *hEGFR* cDNA will be inserted into the first exon of the mouse *Egfr* gene (black box) and placed under the control of the endogenous mouse *Egfr* promoter. This correctly targeted allele will be referred to as the *hEGFR* knock-in allele (*hEGFR*^{KI}). The neomycin resistance gene (*RSV-neo*) and the thymidine kinase gene (*HSV-tk*) are shown. The broken lines delineate the homology regions in the targeting vector, the horizontal bar indicates the Southern blot probe, and the black arrowheads indicate the PCR primers employed for genotype analysis. X, *Xba*I; BX, *Bst*XI; N, *Nde*I. (B) PCR analysis of genomic DNA isolated from the progeny of *hEGFR*$^{KI/+}$ intercrosses. (C) Photograph of 6-week-old *hEGFR*$^{KI/KI}$ and littermate control mice showing that *hEGFR*$^{KI/KI}$ mice are smaller and display short fur hair. (D) Weight representative of a *hEGFR*$^{KI/KI}$ and control littermate mouse at different postnatal ages. At all stages, *hEGFR*$^{KI/KI}$ mice are significantly smaller than their littermates. w, weeks; m, months

(Fig. 1B). Although no viable *hEGFR*$^{KI/KI}$ mice were obtained in a 129/Sv background (0/68), ~7% of *hEGFR*$^{KI/KI}$ mice were born alive in a mixed 129/Sv×C57BL/6 background (Fig. 1C). When bred with *Egfr*$^{+/-}$ mice, no viable *hEGFR*$^{KI/-}$ mice could be obtained, even in the mixed 129/Sv×C57BL/6 background, indicating that one copy of the *hEGFR*^{KI} allele is not sufficient to rescue the lethality of *Egfr*$^{-/-}$ mice (data not shown). Therefore, the phenotypic analysis was performed on surviving *hEGFR*$^{KI/KI}$ mice of mixed 129/Sv×C57BL/6 background, which at birth could be identified by their open eyes and curly whiskers (data not shown). The development of the first coat hair was delayed and the hair was generally much shorter and sparse (Fig. 1C). Some of the *hEGFR*$^{KI/KI}$ mice survived up to 7 months after birth, but were always significantly smaller than their control littermates (Fig. 1C,D). These observations strongly suggest that the *hEGFR*^{KI} allele is most probably not efficiently expressed leading to a hypomorphic phenotype.

Expression analysis in *hEGFR*$^{KI/KI}$ mice

To compare the expression levels of the *hEGFR*^{KI} allele to the endogenous mouse *Egfr*, total RNA was extracted from various organs of a *hEGFR*$^{KI/+}$ heterozygous mouse. Ribonuclease (RNAse) protection assay was performed using a riboprobe, which recognises both the endogenous and the *hEGFR*^{KI} transcripts, but the respective protected bands are different in size. Surprisingly, the *hEGFR*^{KI} allele was not expressed at lower levels than the endogenous *Egfr* in every tissue (Fig. 2A). Organs, which are mostly composed of epithelial cells such as liver, lung, skin and stomach expressed significantly lower levels of the *hEGFR*^{KI} allele compared with the endogenous allele (Fig. 2A). By contrast, in brain regions such as cortex and hippocampus, in kidney and in thymus the *hEGFR*^{KI} allele was expressed at similar levels as the endogenous mouse allele (Fig. 2A). Interestingly, in the heart the *hEGFR*^{KI} allele seemed to be expressed at even higher levels than the endogenous one (Fig. 2A). These results suggest that the *hEGFR*^{KI} allele behaves like a hypomorph particularly in epithelial tissues.

To investigate the expression of the *hEGFR*^{KI} allele at the protein level, lysates were prepared from brain, liver and heart of *hEGFR*$^{KI/KI}$, *hEGFR*$^{KI/+}$, *Egfr*$^{+/+}$ and *Egfr*$^{-/-}$ mice. Western blot analysis employing an anti-EGFR antibody recognising both the mouse and the human EGFR protein showed that EGFR protein of similar size was produced in the brain and liver of wild-type and *hEGFR*$^{KI/KI}$ mice (Fig. 2B). The levels of EGFR protein expressed in the brain were similar to controls, but severely reduced in the liver of *hEGFR*$^{KI/KI}$ mice correlating with the mRNA expression results (Fig. 2A,B). An in vitro EGFR autophosphorylation assay, which is usually more sensitive than western blot analysis, was performed on immunoprecipitated EGFR complexes. Consistent with the previous results, EGFR protein levels were similar to control in the brain of *hEGFR*$^{KI/KI}$ mice, whereas they were lower and almost absent in the liver (Fig. 2C). Using both assays, EGFR protein could not be detected in the hearts of all mice analysed, most probably owing to very low EGFR levels (Fig. 2C and data not shown).

Rescue of the brain phenotypes in *hEGFR*$^{KI/KI}$ mice

In the brain, the *hEGFR*^{KI} allele is expressed at similar levels

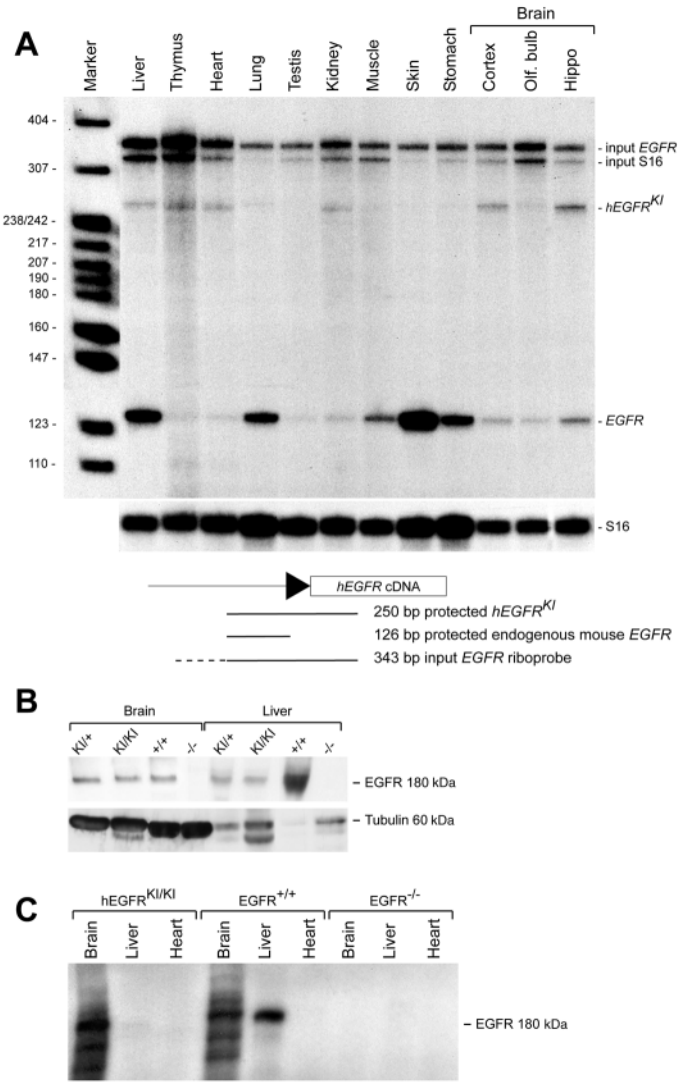

Fig. 2. The *hEGFR*^{KI} allele is not efficiently expressed in epithelial tissues. (A) Expression of the endogenous mouse *Egfr* and the *hEGFR*^{KI} mRNAs measured by RNAse protection assay. The analysis was performed on total RNA isolated from various organs of a heterozygote *hEGFR*$^{KI/+}$ male mouse employing an antisense *Egfr* riboprobe, which detects both the endogenous mouse *Egfr* and the *hEGFR*^{KI} transcripts. In addition to 93 bp of nonspecific sequence (broken line), this riboprobe encompasses the region of the *hEGFR*^{KI} allele bridging the *Egfr* mouse promoter, the loxP site and the 5′ end of the *hEGFR* cDNA. The input probe and the protected fragments are depicted schematically and the black triangle indicates the loxP site. A mouse S16 riboprobe (lower panel) was used as an internal control for equal sample loading in each lane. (B) Western blot analysis showing EGFR protein expression in brain and liver of mice of different genotypes. Immunoblotting was performed on total protein extracts using an anti-EGFR antibody recognising human and mouse EGFR and anti-tubulin was used as a control for protein loading. (C) In vitro EGFR autophosphorylation assay measuring EGFR protein levels. Prior to the kinase assay, protein lysates from various organs were immunoprecipitated with an anti-EGFR antibody recognising both the mouse and the human EGFR protein. Equal loading of protein was verified by Coomassie Blue staining (data not shown)

than the endogenous *Egfr* (Fig. 2A). In order to investigate whether in *hEGFR*$^{KI/KI}$ mice the brain phenotypes were rescued, brains were isolated at different stages after birth and compared to *Egfr*$^{-/-}$ and controls. At all stages analysed, brains of *hEGFR*$^{KI/KI}$ mice appeared structurally normal and comparable to controls (Fig. 3A,B). Histological sections through the frontal cortex of a 3-month-old *hEGFR*$^{KI/KI}$ mouse did not reveal any signs of degeneration and apoptosis and the cortical tissues appeared normal and comparable to controls (Fig. 3C,E). By contrast, in the cortex of *Egfr*$^{-/-}$ mice morphological changes consisting of nuclear condensations and diminished cell densities could be observed already at postnatal day 7 (Fig. 3G) (Sibilia et al., 1998). Similar to controls, in hippocampal sections of *hEGFR*$^{KI/KI}$ mice no ectopic neurones could be observed at any stage, whereas in *Egfr*$^{-/-}$ mice nests of ectopic neurones were always present (Fig. 3D,F,H) (Sibilia et al., 1998). In addition, other brain regions such as the olfactory bulb, thalamus and cerebellum of *hEGFR*$^{KI/KI}$ mice appeared normal and comparable with controls (data not shown).

We next isolated astrocytes from the frontal cortex of newborn *hEGFR*$^{KI/KI}$ mice and analysed their proliferation potential in vitro. As shown in Fig. 3I, the proliferation rate of *hEGFR*$^{KI/KI}$ primary astrocytes was comparable with *hEGFR*$^{KI/+}$ and *Egfr*$^{+/+}$ astrocytes. As the *hEGFR*^{KI} allele is flanked by loxP sites, the *hEGFR* was deleted by breeding *hEGFR*$^{KI/KI}$ mice to *GFAP-cre* transgenic mice, which express the Cre recombinase in astrocytes (Marino et al., 2000). Removal of the EGFR severely compromised the proliferation capacity of primary astrocytes and after 42 days in culture their cumulative cell number reached only about 15% of the values obtained with *hEGFR*$^{KI/KI}$ and control astrocytes (Fig. 3I). Overall, the proliferation rate of *hEGFR*$^{KI/KI}$ *GFAP-cre* astrocytes was reduced to the same extent as in *Egfr*$^{-/-}$ astrocytes (Fig. 3I) (Sibilia et al., 1998). Southern blot analysis confirmed the absence of the *Egfr* gene in *hEGFR*$^{KI/KI}$ *GFAP-cre* astrocytes (Fig. 3J). These results indicate that expression of the *hEGFR*^{KI} allele is fully rescuing the brain and astrocyte defects of *Egfr*$^{-/-}$ mice.

Severe hair follicle and hair cycle defects in *hEGFR*$^{KI/KI}$ mice

The *hEGFR*^{KI} allele is not efficiently expressed in the skin based on the RNAse protection analysis (Fig. 2A). Moreover, *hEGFR*$^{KI/KI}$ mice displayed curly whiskers and the development of the first coat hair was impaired (Fig. 1C). These phenotypes greatly resemble the ones observed in *Egfr*$^{-/-}$ mice (Miettinen et al., 1995; Sibilia and Wagner, 1995; Threadgill et al., 1995). However, in contrast to *Egfr*$^{-/-}$ mice, which do not survive longer than postnatal day 20, *hEGFR*$^{KI/KI}$ mice survive up to 6 months after birth and, therefore, represent a useful model to analyse how reduced EGFR expression affects hair development. The skin of *hEGFR*$^{KI/KI}$ mice was isolated postnatally at different stages of the hair cycle, after 18 days (end of first cycle, catagen/early telogen), after 1 month (second cycle, end of anagen/early catagen) and after 3 months (resting phase, telogen). Histological examination of *hEGFR*$^{KI/KI}$ skins showed

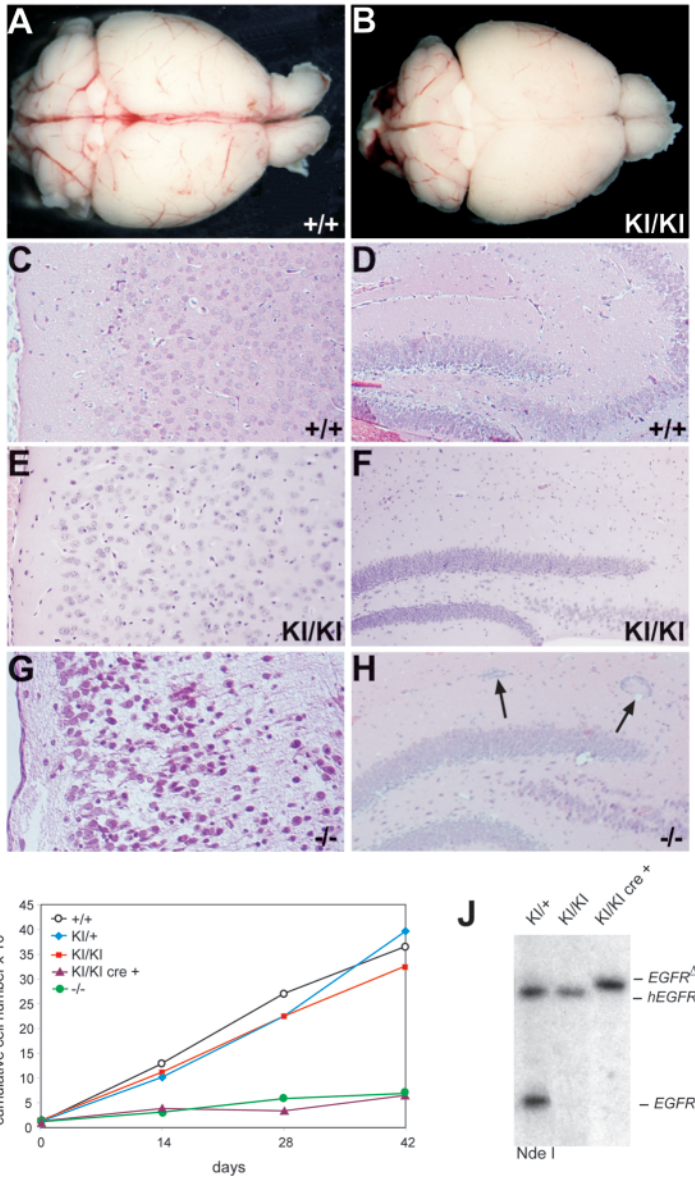

Fig. 3. Normal brain development in *hEGFR*$^{KI/KI}$ mice. Dorsal view of the brains of control (A) and *hEGFR*$^{KI/KI}$ mice (B) isolated 3 months after birth. Histological sections through the frontal cortex (C,E) and hippocampus (D,F) of control (C,D) and *hEGFR*$^{KI/KI}$ (E,F) brains showing normal architecture and morphology. (G,H) Sections of *Egfr*$^{-/-}$ brains show neuronal degeneration in the cortex (G), starting around postnatal day 5, and groups of ectopic neurones (arrows) in the white matter of the hippocampus (H, arrows) (Sibilia et al., 1998). (C-H) Sections are stained with Haematoxylin and Eosin. (I) Cumulative cell number of *Egfr*$^{+/+}$, *hEGFR*$^{KI/+}$, *hEGFR*$^{KI/KI}$, *hEGFR*$^{KI/KI}$ *GFAP-Cre* and *Egfr*$^{-/-}$ primary cortical astrocytes isolated from newborn brains showing that *hEGFR*$^{KI/KI}$ astrocytes display a normal proliferation capacity. Removal of the *hEGFR*^{KI} allele in astrocytes of *hEGFR*$^{KI/KI}$ *GFAP-cre* mice results in severe proliferation defects as observed in *Egfr*$^{-/-}$ astrocytes. (J) Southern blot analysis of genomic DNA isolated from astrocytes shown in I and hybridised with the probe shown in Fig. 1A. The bands corresponding to the different alleles are indicated. *EGFR*$^{\Delta}$: *hEGFR*^{KI} allele after Cre-mediated deletion.

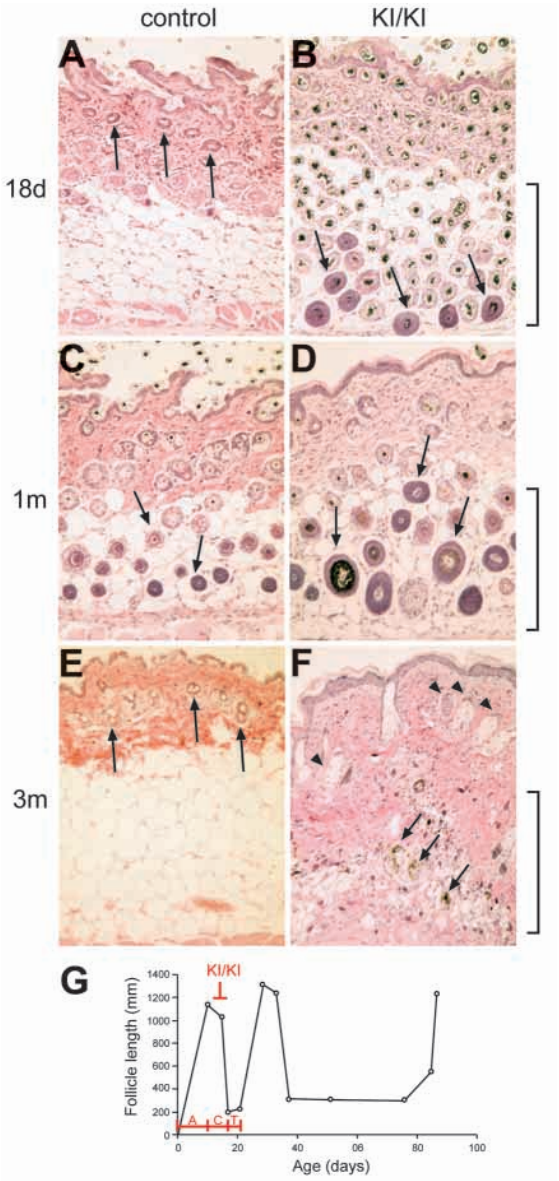

Fig. 4. Impaired hair cycle and follicle development in *hEGFR*$^{KI/KI}$ mice. Histological sections through the skin of control (A,C,E) and *hEGFR*$^{KI/KI}$ mice (B,D,F) at different stages of the hair cycle. In control skins at 18 days (end of catagen/telogen) the hair follicles are confined to the upper dermal layers (A, arrows), whereas in *hEGFR*$^{KI/KI}$ skins, hair follicles accumulate in the subdermal fat tissue (brackets in B,D,F), as they do not progress from anagen to telogen (B). Arrows in B indicate hair follicles that start to be enlarged in mutant skins. (C) At 1 month (late anagen/early catagen) control follicles are distributed in the upper dermal and subdermal fat layers and display a normal structure (arrows). (D) Mutant follicles in the subdermal fat tissue are severely hyperplastic (arrows) at this stage. (E) At 3 months (telogen), control follicles are confined to the upper dermal layers (arrows). (F) In mutant skins, only a few aberrant follicles are present in the upper dermis (arrowheads) and most of the follicles stuck in the subdermal fat tissue have degenerated (arrows). Severe fibrosis with infiltration of inflammatory cells can be detected in the subdermal fat tissue of *hEGFR*$^{KI/KI}$ skins as evidenced by the strong eosin (pink) staining. (G) A normal mouse hair cycle profile with the position where the hair cycle is blocked in *hEGFR*$^{KI/KI}$ mice. A, anagen; C, catagen; T, telogen; d, days; m, months. All sections are stained with Haematoxylin and Eosin.

striking alterations in the morphology and distribution of hair follicles. Around day 18, hair follicles of control mouse skin go through a telogen stage and are confined to the upper layer of the dermis (Fig. 4A). By contrast, at this stage follicles of *hEGFR*$^{KI/KI}$ mice were still much longer reaching deep into the subdermal adipose tissue, suggesting that they had failed to enter into catagen and were still in anagen (Fig. 4B,G). *hEGFR*$^{KI/KI}$ follicles started to appear much larger and hyperplastic compared with control follicles and this phenotype was even more pronounced at 1 month when the anagen of the second hair cycle had started (Fig. 4C,D). After completion of the second hair cycle, follicles remain for a long period (around 40 days) in telogen (Fig. 4G). During this stage (at the age of 3 months), control hair follicles are short and localised in the upper layers of the dermis (Fig. 4E). By contrast, in *hEGFR*$^{KI/KI}$ mice, only very few structurally abnormal follicles were present in the upper dermis and most of the follicles, which had remained stuck in the subdermal fat layers, were degenerated (Fig. 4F). The cell layers composing the hair follicles were very thin and partly destroyed (Fig. 4F). Severe fibrosis of the dermis and subdermal fat tissue with massive infiltration of inflammatory cells was observed and had most likely been triggered by the exposure of naked hair shafts from the degenerating follicles (Fig. 4F and data not shown). The inflammatory infiltrate mainly contained macrophages, lymphocytes, neutrophils and multinucleated giant cells (data not shown). The progressive degeneration and inflammation led to the loss of most follicles over time and the majority of *hEGFR*$^{KI/KI}$ mice were completely bald at the age of 5-7 months (data not shown). These results indicate that EGFR signalling is absolutely required for hair cycle progression. Moreover, EGFR is also essential for proper hair follicle differentiation, orientation and migration, as well as to preserve hair follicle integrity during the hair cycle.

Bone cell defects in *hEGFR*$^{KI/KI}$ mice

hEGFR$^{KI/KI}$ and *Egfr*$^{-/-}$ mice are significantly smaller than their control littermates. Impaired skeletal development is one of several defects that can be responsible for growth retardation. Therefore, we investigated whether bone development was defective in *hEGFR*$^{KI/KI}$ mice. Histological analysis of the long bones at birth revealed that the hypertrophic chondrocyte zone of the growth plate was significantly increased in *hEGFR*$^{KI/KI}$ mice (Fig. 5A,B). This phenotype might be caused either by increased or reduced expression of the *hEGFR*^{KI} allele in the bone compartment. To discriminate between these two possibilities, bone sections from *Egfr*$^{-/-}$ newborn mice of mixed genetic background were analysed. Interestingly, in *Egfr*$^{-/-}$ long bones the zone of hypertrophic chondrocytes was similarly or even more increased as in *hEGFR*$^{KI/KI}$ bones, indicating that this phenotype is most probably caused by the absence of EGFR expression in cartilage (Fig. 5B,C). The proliferation of chondrocytes measured by Ki67 staining on sections was not affected and comparable in all three genotypes (Fig. 5E). The expression of EGFR in chondroblasts was analysed by X-galactosidase staining in *Egfr*$^{+/-}$ E14.5 foetuses, as the knockout allele harbours an *E. coli lacZ* gene inserted in-frame downstream of the first exon of the mouse *Egfr* gene (Sibilia and Wagner, 1995). In control foetuses, EGFR expression was detected in chondroblasts of all ossification centres (Fig. 5D). These results show that EGFR is expressed in chondroblasts during

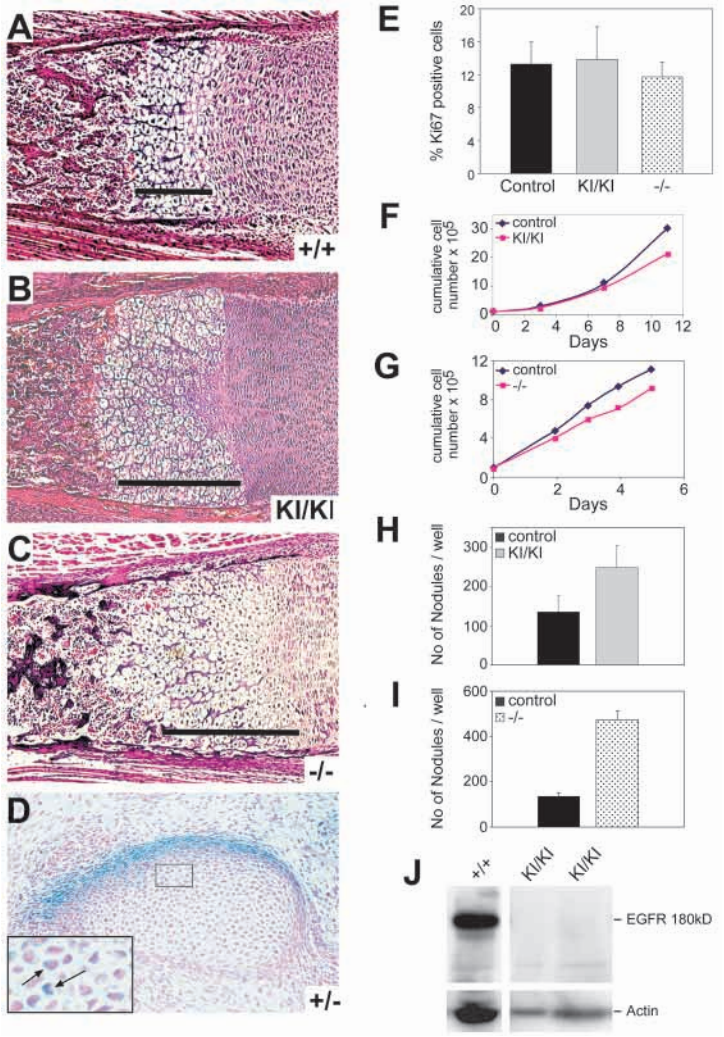

Fig. 5. Bone cell defects in the absence of EGFR. Histological sections through the tibiae of control (A), *hEGFR*$^{KI/KI}$ (B) and *Egfr*$^{-/-}$ mice (C) at postnatal day 1. The black bar marks the zone of hypertrophic chondrocytes, which is markedly increased in both *hEGFR*$^{KI/KI}$ and *Egfr*$^{-/-}$ long bones. (D) X-galactosidase (X-gal) staining of an E14.5 *Egfr*$^{+/-}$ foetus showing EGFR expression (blue stain) in the ossification center of the vertebrae. Inset shows a higher magnification of the region boxed in D with arrows indicating X-gal staining in chondroblasts. (A-C) Haematoxylin and Eosin staining; (D) X-gal and Eosin staining. (E) The proliferation of chondrocytes was measured by Ki67 staining on bone sections of mice of the indicated genotypes. The data represent the mean±s.d. of the number of Ki67-positive chondrocytes present on six different sections. (F,G) Cumulative cell number of *hEGFR*$^{KI/KI}$ (F) and *Egfr*$^{-/-}$ (G) primary osteoblasts isolated from newborn calvariae showing reduced proliferation of *hEGFR*$^{KI/KI}$ and *Egfr*$^{-/-}$ osteoblasts at the end of the culture period. (H,I) Primary osteoblasts derived from *hEGFR*$^{KI/KI}$ (H) and *Egfr*$^{-/-}$ (I) neonatal calvariae showed enhanced bone nodule formation compared with controls. Data represent the mean±s.e.m. (J) Western blot analysis showing EGFR (180 kDa) protein expression in *hEGFR*$^{KI/KI}$ and control osteoblasts. Anti-Actin immunoblotting was used as an internal protein loading control.

development and suggest that EGFR signalling negatively regulates the maturation of hypertrophic chondrocytes, because the zone of hypertrophic chondrocytes is enlarged in its absence.

To test whether loss of the EGFR also influences osteoblastic differentiation and proliferation, calvarial osteoblasts were prepared from newborn *hEGFR*$^{KI/KI}$, *Egfr*$^{-/-}$ and control mice. The proliferation potential of *hEGFR*$^{KI/KI}$ and *Egfr*$^{-/-}$ primary calvarial osteoblasts was decreased towards the end of the culture period (Fig. 5F,G). Moreover, calvarial osteoblasts derived from *hEGFR*$^{KI/KI}$ and *Egfr*$^{-/-}$ mice showed increased differentiation compared to controls, as assessed by an in vitro mineralisation assay. Compared with controls, *hEGFR*$^{KI/KI}$ and *Egfr*$^{-/-}$ osteoblast cultures formed approximately twice and three times as many mineralised bone nodules, respectively (Fig. 5H,I). Western blot analysis revealed a severe reduction of EGFR expression in calvarial osteoblasts of *hEGFR*$^{KI/KI}$ mice (Fig. 5J). Although differentiation and proliferation defects were observed in cultured osteoblasts, the bone thickness of newborn *hEGFR*$^{KI/KI}$ and *Egfr*$^{-/-}$ mice was comparable with controls and no overt bone remodelling defects could be detected (Fig. 5A-C). These results suggest that EGFR signalling normally supports proliferation, but inhibits differentiation of osteoblastic cells, keeping them in an undifferentiated, pre-osteoblastic state.

hEGFR$^{KI/KI}$ mice develop heart hypertrophy

hEGFR$^{KI/KI}$ mice can survive up to 6 months after birth, but often sudden death is observed at earlier times. To investigate the possible cause of lethality, *hEGFR*$^{KI/KI}$ mice were sacrificed and different organ systems were analysed. An increase in heart size was consistently observed, which was already visible at 3 weeks after birth and became more pronounced with age (Fig. 6A). Comparison of heart weights at 3 months of age showed that *hEGFR*$^{KI/KI}$ hearts were about twice as heavy as control *hEGFR*$^{KI/+}$ and *EGFR*$^{+/+}$ hearts (Fig. 6B). This difference was even more dramatic when the heart weights were corrected for the body weights considering that *hEGFR*$^{KI/KI}$ mice are smaller and only about half of the size of control mice (Fig. 6B). Histological cross-sections through the hearts of *hEGFR*$^{KI/KI}$ mice revealed a severe hypertrophy with dramatically increased thickness of the left ventricular wall and the interventricular septum at 3 weeks after birth (Fig. 6D). These defects became more severe with increasing age (Fig. 6G). Cardiomyocytes of 2.5- to 3.5-month-old *hEGFR*$^{KI/KI}$ mice were hypertrophic and measurements of their mean cross-sectional areas revealed a 1.9-fold increase compared with controls (mean cross sectional area±s.d.: 309.7±97.6 μm^2 versus 166.3±16.3 μm^2). None of these defects was ever observed in control *hEGFR*$^{KI/+}$ and *Egfr*$^{+/+}$ mice (Fig. 6C,F; data not shown). In 3-week-old *Egfr*$^{-/-}$ mice, the heart size was normal, the heart-to-body weight ratios were comparable with controls and histological sections did not reveal signs of hypertrophy (Fig. 6E; data not shown). Cardiac hypertrophies can occur as primary myocardial diseases or as a consequence of other conditions such as valve defects leading to valvular stenosis and/or regurgitation (Katz, 1990). When compared with controls, histological examinations of *hEGFR*$^{KI/KI}$ hearts revealed that the cusps of the pulmonary and aortic valves were thickened and hypercellular, a condition that most likely resulted from the

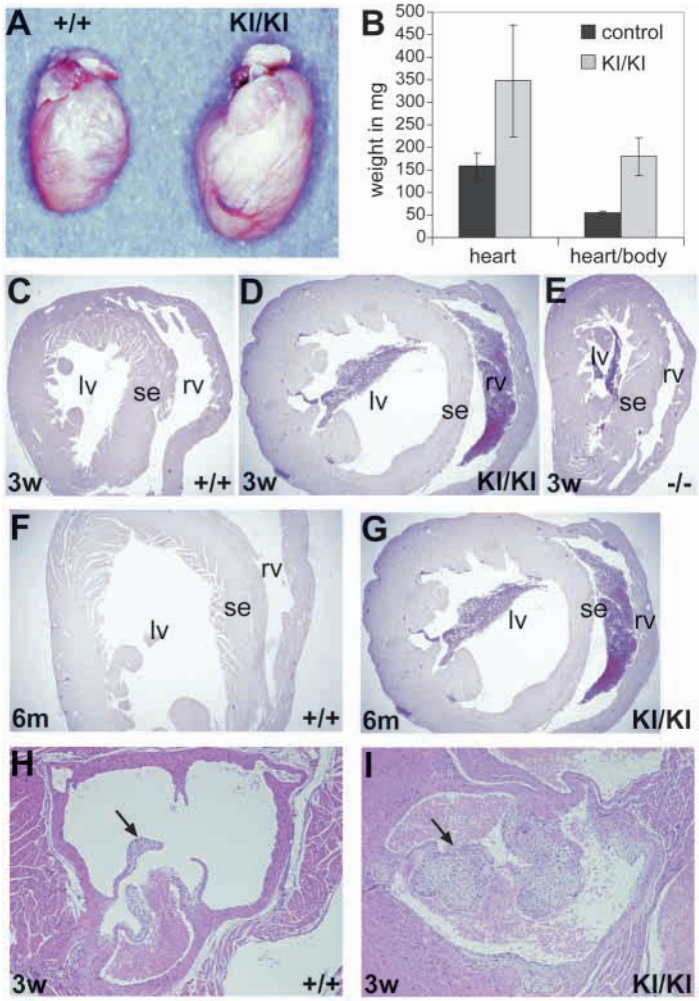

Fig. 6. Heart hypertrophy and semilunar valve defects in *hEGFR*$^{KI/KI}$ mice. (A) Appearance of control and *hEGFR*$^{KI/KI}$ hearts at 3 weeks of age. (B) Heart weights and relative heart weights corrected for body weight of control and *hEGFR*$^{KI/KI}$ mice. Data represent the mean±s.d. of five 3-month-old mice and hearts. Cross-sections through the heart of control (C,F), *hEGFR*$^{KI/KI}$ (D,G) and *Egfr*$^{-/-}$ (E) mice at different postnatal stages, showing severe myocardial hypertrophy in *hEGFR*$^{KI/KI}$ mice. lv, left ventricle; se, septum; rv, right ventricle. Histological sections of semilunar valves from control (H) and *hEGFR*$^{KI/KI}$ (I) hearts. The arrows in H and I indicate the aortic valve leaflets, which are thickened and hypercellular in *hEGFR*$^{KI/KI}$ hearts. w, weeks; m, months. All sections are stained with Haematoxylin and Eosin.

accumulation of mesenchymal cells (Fig. 6H,I). By contrast, the atrioventricular valves were not affected and appeared normal (data not shown). The same semilunar valve defects as in *hEGFR*$^{KI/KI}$ hearts were also observed in *Egfr*$^{-/-}$ mice (data not shown) indicating that these defects result from the absence of expression of the EGFR in valve structures. As *Egfr*$^{-/-}$ mice do not display severe myocardial hypertrophy, these results suggest that in *hEGFR*$^{KI/KI}$ mice the semilunar valve defects together with the increased expression of the *hEGFR*^{KI} allele in the myocardium (Fig. 2A) exacerbate the heart hypertrophy thereby contributing to increased lethality of the mice.

Discussion

In this study, a knock-in approach was employed to generate humanised EGFR mice, which harbour a human *EGFR* cDNA flanked by loxP sites. *hEGFR*$^{KI/KI}$ mice display tissue-specific hypomorphic phenotypes, which correlate with the expression levels of the *hEGFR*^{KI} allele in various tissues. This is surprising because other genetically engineered alleles that displayed hypomorphic behaviour showed reduced expression in most of the tissues analysed (Vivian et al., 1999). Often hypomorphic alleles still harbour the neomycin resistance cassette with its regulatory elements in the locus and it has been shown for several genes that this can interfere with their proper expression in many tissues (Meyers et al., 1998; Partanen et al., 1996). This is a likely explanation for the low expression of the *hEGFR*^{KI} allele as it also contains a neomycin cassette in the first intron downstream of the human *EGFR* cDNA. The surprising finding, however, is that the *hEGFR*^{KI} allele is not hypomorphic in every tissue, but only in bone and epithelial cells. In other organs such as the brain the expression levels of the *hEGFR*^{KI} allele were comparable with the endogenous mouse *Egfr* gene. This suggests that there might be elements regulating *Egfr* expression in a tissue-specific manner. It is possible that the controlling elements of the neomycin gene interfere and compete with transcription factors, which would otherwise direct correct *EGFR* expression in the affected organs. Alternatively, the insertion of the human *EGFR* cDNA into the mouse locus might alter its chromatin conformation, thereby rendering it inaccessible to tissue-specific transcription factors.

In all the brain regions analysed, the *hEGFR*^{KI} allele was expressed at similar levels to the endogenous mouse gene. In fact, in brains of homozygote *hEGFR*$^{KI/KI}$ mice none of the defects observed in *Egfr*$^{-/-}$ mice could be detected. *hEGFR*$^{KI/KI}$ mice do not develop the cortical neurodegeneration and astrocyte proliferation in vitro is comparable with controls. Only after Cre-mediated deletion of the floxed *hEGFR*^{KI} allele a severe proliferation defect was observed in astrocytes cultured in vitro, demonstrating that the EGFR is required for proper proliferation of these cells. *hEGFR*$^{KI/KI}$ mice did also not contain ectopic neurones in the hippocampus, a phenotype that is always observed in *Egfr*$^{-/-}$ mice (Sibilia et al., 1998). Because all the brain defects observed in *Egfr*$^{-/-}$ mice were rescued in *hEGFR*$^{KI/KI}$ mice, it can be assumed that the amount of EGFR protein present in brain cells of *hEGFR*$^{KI/KI}$ mice is similar to that in wild-type controls. Moreover, it appears that the binding affinity of the mouse EGFR ligands to the human EGFR is not significantly altered, suggesting that impaired receptor activation is not contributing to the hypomorphic defects seen in other tissues.

The observed phenotypes are probably determined by the level of transcription of the *hEGFR*^{KI} allele in various tissues. In epithelial tissues such as the skin and hair follicles where the *hEGFR*^{KI} allele is poorly transcribed, severe defects were observed that resemble those observed in *Egfr*$^{-/-}$ mice (Miettinen et al., 1995; Sibilia and Wagner, 1995; Threadgill et al., 1995). Because *Egfr*$^{-/-}$ mice do not survive longer than P20, the skin and hair phenotypes could not be properly analysed directly in mutant mice. The *hEGFR*$^{KI/KI}$ mice proved

to be extremely useful to analyse how the absence of the EGFR affects hair follicle differentiation, migration and cycling. After the first hair cycle, hair follicles of *hEGFR*$^{KI/KI}$ mice fail to enter into catagen and remain in aberrant anagen, indicating that EGFR signalling is needed to regulate hair cycle progression. The EGFR also seems to be required to preserve hair follicle integrity over time, because in its absence the follicles are degraded probably by the infiltrating inflammatory cells. The aberrant localisation of *hEGFR*$^{KI/KI}$ hair follicles in the skin might have triggered an immunological response, which results in the destruction of the follicles. Alternatively, as the EGFR has been shown to inhibit differentiation and promote survival of epithelial cells, it is possible that in the absence of EGFR expression, hair follicles might be impaired in their survival capacity and/or undergo premature differentiation. With time, this would lead to hair follicle destruction and release of follicle material into the dermis, which in turn would trigger the immunological response. Similar hair abnormalities have also been observed in grafting experiments with *Egfr*$^{-/-}$ skin onto immunodeficient mice and in a skin targeted DN *Egfr* transgenic mouse model (Hansen et al., 1997; Murillas et al., 1995). However, in the latter model it could not be excluded that the severity of the phenotypes observed was determined not only by inhibition of the EGFR itself but also by the inhibition of the other Erbb family members which are also expressed in the epidermis (Stoll et al., 2001). As the skin and hair follicle defects observed in *hEGFR*$^{KI/KI}$ and the DN *EGFR* transgenic mice are very similar, it can be concluded that these phenotypes mainly result from direct EGFR inhibition.

EGFR signalling does not only seem to inhibit epithelial cell differentiation, but also the differentiation of bone cells. Bone development starts with the formation of mesenchymal condensations that first differentiate into chondrocytes, which become hypertrophic and are then invaded by blood vessels, bone-forming osteoblasts and bone-resorbing osteoclasts (Karsenty and Wagner, 2002). Active remodelling ultimately gives rise to a bone with growth plate and a central marrow cavity (Karsenty and Wagner, 2002). Numerous extracellular factors, such as hormones, growth factors and cytokines, modulate bone remodelling via differentiation and proliferation of bone cells, and this process has to be tightly regulated in order to prevent bone diseases (Karsenty and Wagner, 2002). The EGFR is expressed in chondroblasts of the developing ossification centres and the EGFR has also been shown to be expressed in osteoblasts and osteocytes in vivo (Davideau et al., 1995). However, no bone defects have been reported so far for mice defective in EGFR signalling. A recent report has shown that transgenic mice expressing EGF ubiquitously are growth retarded, display defective chondrocyte development in the growth plate and osteoblasts accumulate in the endosteum and periosteum (Chan and Wong, 2000). Controversial in vitro data regarding the role of EGFR signalling in bone cells have been reported, although two studies suggest that EGFR might stimulate osteogenic cell proliferation and suppress the differentiation into mature osteoblasts and chondrocytes (Chien et al., 2000; Yoon et al., 2000). In *Egfr*$^{-/-}$ and *hEGFR*$^{KI/KI}$ mice both osteoblasts and chondrocytes display increased differentiation in vitro and in vivo, respectively. As the *hEGFR*^{KI} allele was poorly expressed in the affected cell types, it is likely that these defects result from the lack of *Egfr* expression. In the long bones of *hEGFR*$^{KI/KI}$ mice, the region of hypertrophic chondrocytes in the growth plate was significantly increased, suggesting that chondrocytes had undergone premature differentiation. This phenotype was even more severe in *Egfr*$^{-/-}$ mice, where *Egfr* expression is completely absent, indicating that EGFR signalling prevents differentiation of chondrocytes. Although no overt differences in bone mass could be detected in newborn *Egfr*$^{-/-}$ and *hEGFR*$^{KI/KI}$ mice, calvarial osteoblasts from these mice proliferate more slowly and display an increased differentiation capacity in vitro. It is likely that EGFR signalling is important to keep osteoblasts and chondrocytes in a proliferative state and inhibit their differentiation, thus allowing proper development of long bones. In the absence of EGFR expression, accelerated differentiation of chondrocytes and possibly decreased proliferation of osteoblasts can disturb longitudinal growth of long bones leading to severe growth retardation in the mice.

hEGFR$^{KI/KI}$ mice develop a severe heart hypertrophy with dramatically increased thickness of the ventricular walls and the interventricular septum, which was visible already at 3 weeks after birth and became more pronounced as age proceeded. Interestingly, *Egfr*$^{-/-}$ mice did not display signs of hypertrophy at this age, suggesting that this phenotype was most probably not due to the lack of EGFR expression. Cardiac hypertrophy is an adaptive response to many forms of disorders such as hypertension, myocardial infarction and valve defects aimed to augment the cardiac output (Katz, 1990). However, sustained hypertrophy usually leads to ventricular dilatation with consequent heart failure and sudden death (Katz, 1990). The response of cardiomyocytes to hypertrophic signals involves an increase in cell size and protein synthesis, induction of immediate-early genes such as AP-1 and re-expression of several foetal myocardial structural proteins (Sadoshima and Izumo, 1997). It has been shown that treatment of rat cardiomyocytes with EGF can trigger a hypertrophic response resulting in increased protein synthesis and transcriptional activation of *Fos* and *Jun* (Rebsamen et al., 2000). Similarly, G-protein-coupled receptor (GPCR) agonists were shown to transactivate the EGFR via shedding of HB-EGF by the metalloproteinase ADAM12 thereby inducing heart hypertrophy (Asakura et al., 2002; Prenzel et al., 1999). Moreover, EGF increases adenyl cyclase activity and cAMP accumulation, thus enhancing the heart contractility and beating rate (Nair et al., 1993). As heart-specific expression of the *hEGFR*^{KI} allele seemed to be slightly higher than the endogenous wild-type allele, we speculate that increased EGFR signalling in cardiomyocytes is contributing to the development of the heart hypertrophy.

hEGFR$^{KI/KI}$ mice also display semilunar valve defects, which are known to induce aortic stenosis and regurgitation, and as a consequence can lead to heart hypertrophy. Heart valves develop from the endocardium, a specialised endothelium that undergoes complex epithelial-mesenchymal transformations leading to the formation of mesenchymal outgrowths (also called the cardiac cushions), from which the mature valve leaflets originate (Towbin and Belmont, 2000). The pulmonary and aortic, but not the atrioventricular valves of *hEGFR*$^{KI/KI}$ hearts were thickened and hypercellular, which most probably results from the accumulation of mesenchymal cells. As similar valve defects were also present in *Egfr*$^{-/-}$ hearts, it is likely that

the *hEGFR*^{KI} allele is not expressed in the developing valves. Although we were unable to detect EGFR expression in wild-type valve structures by immunohistochemistry, we believe that the valve defects of *hEGFR*$^{KI/KI}$ and *Egfr*$^{-/-}$ hearts result from lack of EGFR expression in these structures. The other EGFR family members Erbb2 and Erbb4 are expressed in the endocardium and have been shown to be involved in the formation of the mesenchymal cushions (Camenisch et al., 2002; Erickson et al., 1997). It still remains to be determined how EGFR alone or in combination with these receptors regulates mesenchyme development and its differentiation into mature valve structures.

By studying the genetic interaction between EGFR and the protein-tyrosine phosphatase Shp2, it was shown that EGFR is required for semilunar valve development (Chen et al., 2000). Compound mutants between Shp2 and the hypomorphic *EGFR*$^{wa2/wa2}$ mouse strains showed signs of aortic stenosis and regurgitation with subsequent development of myocardial hypertrophy (Chen et al., 2000). Although these defects were most severe in compound mutants, thickened semilunar valves were also observed in *EGFR*$^{wa2/wa2}$ and *Egfr*$^{-/-}$ mice, whereas no cardiac dilatation were reported for the single EGFR mutants (Chen et al., 2000). Similarly, we could not detect any signs of myocardial hypertrophy in 3-week-old *Egfr*$^{-/-}$ mice, although semilunar valve thickening was observed. By contrast, the heart of *hEGFR*$^{KI/KI}$ mice at this stage was already enlarged and displayed a severe thickening of the myocardial walls. Therefore, it is likely that the severe hypertrophy observed in *hEGFR*$^{KI/KI}$ mice results from the malformations of the valves and from the enhanced hypertrophic response of cardiomyocytes to increased EGFR signalling, as the *hEGFR*^{KI} allele is expressed at higher levels in the myocardium. These defects can lead to a severe heart condition, which is probably responsible for the lethality of *hEGFR*$^{KI/KI}$ mice, whereas the valve defects alone, as seen in *Egfr*$^{wa2/wa2}$ mice do not seem to increase the mortality of these mice. Moreover, as *hEGFR*$^{KI/+}$ mice do not develop heart hypertrophy, it seems unlikely that enhanced expression of the EGFR in the myocardium alone can lead to the development of this heart condition. The conditional *hEGFR*$^{KI/KI}$ mice may provide a useful model not only to study aortic valve diseases and developmental aspects of bone differentiation, but also to test novel therapies aimed to inhibit EGFR signalling for the treatment of cardiac hypertrophies and hyperproliferative bone diseases.

We are grateful to S. Pekez and M. Hammer for maintaining our mouse colonies at IMP and at the Department of Dermatology, respectively. We thank Romeo Ricci for critical reading of the manuscript. B.W. was recipient of a DOC-Fellowship of the Austrian Academy of Sciences. A.H. was funded by EMBO and Marie Curie Individual fellowships. Work in E.F.W.'s laboratory at the IMP is supported by Boehringer Ingelheim and the Austrian Industrial Research Promotion Fund (FFF). Work in M.S.'s laboratory is supported by the Competence Center for Biomolecular Therapeutics (BMT, funded by the Austrian Ministry of Science and Technology, City of Vienna and Industrial Partners) and by the EC program QLG1-CT-2001-00869.

References

Asakura, M., Kitakaze, M., Takashima, S., Liao, Y., Ishikura, F., Yoshinaka, T., Ohmoto, H., Node, K., Yoshino, K., Ishiguro, H. et al. (2002). Cardiac hypertrophy is inhibited by antagonism of ADAM12 processing of HB-EGF: metalloproteinase inhibitors as a new therapy. *Nat. Med.* **8**, 35-40.

Camenisch, T. D., Schroeder, J. A., Bradley, J., Klewer, S. E. and McDonald, J. A. (2002). Heart-valve mesenchyme formation is dependent on hyaluronan-augmented activation of ErbB2-ErbB3 receptors. *Nat. Med.* **8**, 850-855.

Chan, S. Y. and Wong, R. W. (2000). Expression of epidermal growth factor in transgenic mice causes growth retardation. *J. Biol. Chem.* **275**, 38693-38698.

Chen, B., Bronson, R. T., Klaman, L. D., Hampton, T. G., Wang, J. F., Green, P. J., Magnuson, T., Douglas, P. S., Morgan, J. P. and Neel, B. G. (2000). Mice mutant for Egfr and Shp2 have defective cardiac semilunar valvulogenesis. *Nat. Genet.* **24**, 296-299.

Chien, H. H., Lin, W. L. and Cho, M. I. (2000). Down-regulation of osteoblastic cell differentiation by epidermal growth factor receptor. *Calcif. Tiss. Int.* **67**, 141-150.

Davideau, J. L., Sahlberg, C., Thesleff, I. and Berdal, A. (1995). EGF receptor expression in mineralized tissues: an in situ hybridization and immunocytochemical investigation in rat and human mandibles. *Connect Tiss. Res.* **32**, 47-53.

Erickson, S. L., O'Shea, K. S., Ghaboosi, N., Loverro, L., Frantz, G., Bauer, M., Lu, L. H. and Moore, M. W. (1997). ErbB3 is required for normal cerebellar and cardiac development: a comparison with ErbB2-and heregulin-deficient mice. *Development* **124**, 4999-5011.

Fleischmann, A., Hafezi, F., Elliott, C., Reme, C. E., Ruther, U. and Wagner, E. F. (2000). Fra-1 replaces c-Fos-dependent functions in mice. *Genes Dev.* **14**, 2695-2700.

Fowler, K. J., Walker, F., Alexander, W., Hibbs, M. L., Nice, E. C., Bohmer, R. M., Mann, G. B., Thumwood, C., Maglitto, R., Danks, J. A. et al. (1995). A mutation in the epidermal growth factor receptor in waved-2 mice has a profound effect on receptor biochemistry that results in impaired lactation. *Proc. Natl. Acad. Sci. USA* **92**, 1465-1469.

Gassmann, M., Casagranda, F., Orioli, D., Simon, H., Lai, C., Klein, R. and Lemke, G. (1995). Aberrant neural and cardiac development in mice lacking the ErbB4 neuregulin receptor. *Nature* **378**, 390-394.

Hansen, L. A., Alexander, N., Hogan, M. E., Sundberg, J. P., Dlugosz, A., Threadgill, D. W., Magnuson, T. and Yuspa, S. H. (1997). Genetically null mice reveal a central role for epidermal growth factor receptor in the differentiation of the hair follicle and normal hair development. *Am. J. Pathol.* **150**, 1959-1975.

Karsenty, G. and Wagner, E. F. (2002). Reaching a genetic and molecular understanding of skeletal development. *Dev. Cell* **2**, 389-406.

Katz, A. M. (1990). Cardiomyopathy of overload. A major determinant of prognosis in congestive heart failure. *New Engl. J. Med.* **322**, 100-110.

Kornblum, H. I., Hussain, R., Wiesen, J., Miettinen, P., Zurcher, S. D., Chow, K., Derynck, R. and Werb, Z. (1998). Abnormal astrocyte development and neuronal death in mice lacking the epidermal growth factor receptor. *J. Neurosci. Res.* **53**, 697-717.

Lee, K. F., Simon, H., Chen, H., Bates, B., Hung, M. C. and Hauser, C. (1995). Requirement for neuregulin receptor erbB2 in neural and cardiac development. *Nature* **378**, 394-398.

Luetteke, N. C., Phillips, H. K., Qiu, T. H., Copeland, N. G., Earp, H. S., Jenkins, N. A. and Lee, D. C. (1994). The mouse waved-2 phenotype results from a point mutation in the EGF receptor tyrosine kinase. *Genes Dev.* **8**, 399-413.

Luetteke, N. C., Qiu, T. H., Peiffer, R. L., Oliver, P., Smithies, O. and Lee, D. C. (1993). TGF alpha deficiency results in hair follicle and eye abnormalities in targeted and waved-1 mice. *Cell* **73**, 263-278.

Mann, G. B., Fowler, K. J., Gabriel, A., Nice, E. C., Williams, R. L. and Dunn, A. R. (1993). Mice with a null mutation of the TGF alpha gene have abnormal skin architecture, wavy hair, and curly whiskers and often develop corneal inflammation. *Cell* **73**, 249-261.

Marino, S., Vooijs, M., van Der Gulden, H., Jonkers, J. and Berns, A. (2000). Induction of medulloblastomas in p53-null mutant mice by somatic inactivation of Rb in the external granular layer cells of the cerebellum. *Genes Dev.* **14**, 994-1004.

Meyers, E. N., Lewandoski, M. and Martin, G. R. (1998). An Fgf8 mutant allelic series generated by Cre- and Flp-mediated recombination. *Nat. Genet.* **18**, 136-141.

Miettinen, P. J., Berger, J. E., Meneses, J., Phung, Y., Pedersen, R. A., Werb, Z. and Derynck, R. (1995). Epithelial immaturity and multiorgan failure in mice lacking epidermal growth factor receptor. *Nature* **376**, 337-341.

Miettinen, P. J., Chin, J. R., Shum, L., Slavkin, H. C., Shuler, C. F., Derynck, R. and Werb, Z. (1999). Epidermal growth factor receptor function is necessary for normal craniofacial development and palate closure. *Nat. Genet.* **22**, 69-73.

Murillas, R., Larcher, F., Conti, C. J., Santos, M., Ullrich, A. and Jorcano, J. L. (1995). Expression of a dominant negative mutant of epidermal growth factor receptor in the epidermis of transgenic mice elicits striking alterations in hair follicle development and skin structure. *EMBO J.* **14**, 5216-5223.

Nair, B. G., Rashed, H. M. and Patel, T. B. (1993). Epidermal growth factor produces inotropic and chronotropic effects in rat hearts by increasing cyclic AMP accumulation. *Growth Factors* **8**, 41-48.

Olayioye, M. A., Neve, R. M., Lane, H. A. and Hynes, N. E. (2000). The ErbB signaling network: receptor heterodimerization in development and cancer. *EMBO J.* **19**, 3159-3167.

Partanen, J., Puri, M. C., Schwartz, L., Fischer, K. D., Bernstein, A. and Rossant, J. (1996). Cell autonomous functions of the receptor tyrosine kinase TIE in a late phase of angiogenic capillary growth and endothelial cell survival during murine development. *Development* **122**, 3013-3021.

Peus, D., Hamacher, L. and Pittelkow, M. R. (1997). EGF-receptor tyrosine kinase inhibition induces keratinocyte growth arrest and terminal differentiation. *J. Invest. Dermatol.* **109**, 751-756.

Prenzel, N., Zwick, E., Daub, H., Leserer, M., Abraham, R., Wallasch, C. and Ullrich, A. (1999). EGF receptor transactivation by G-protein-coupled receptors requires metalloproteinase cleavage of proHB-EGF. *Nature* **402**, 884-888.

Rebsamen, M. C., Arrighi, J. F., Juge-Aubry, C. E., Vallotton, M. B. and Lang, U. (2000). Epidermal growth factor induces hypertrophic responses and Stat5 activation in rat ventricular cardiomyocytes. *J. Mol. Cell Cardiol.* **32**, 599-610.

Riethmacher, D., Sonnenberg-Riethmacher, E., Brinkmann, V., Yamaai, T., Lewin, G. R. and Birchmeier, C. (1997). Severe neuropathies in mice with targeted mutations in the ErbB3 receptor. *Nature* **389**, 725-730.

Sadoshima, J. and Izumo, S. (1997). The cellular and molecular response of cardiac myocytes to mechanical stress. *Annu. Rev. Physiol.* **59**, 551-571.

Schlessinger, J. (2000). Cell signaling by receptor tyrosine kinases. *Cell* **103**, 211-225.

Sibilia, M. and Wagner, E. F. (1995). Strain-dependent epithelial defects in mice lacking the EGF receptor. *Science* **269**, 234-238.

Sibilia, M., Steinbach, J. P., Stingl, L., Aguzzi, A. and Wagner, E. F. (1998). A strain-independent postnatal neurodegeneration in mice lacking the EGF receptor. *EMBO J.* **17**, 719-731.

Sibilia, M., Fleischmann, A., Behrens, A., Stingl, L., Carroll, J., Watt, F. M., Schlessinger, J. and Wagner, E. F. (2000). The EGF receptor provides an essential survival signal for SOS-dependent skin tumor development. *Cell* **102**, 211-220.

Stoll, S. W., Kansra, S., Peshick, S., Fry, D. W., Leopold, W. R., Wiesen, J. F., Sibilia, M., Zhang, T., Werb, Z., Derynck, R. et al. (2001). Differential utilization and localization of ErbB receptor tyrosine kinases in skin compared to normal and malignant keratinocytes. *Neoplasia* **3**, 339-350.

Threadgill, D. W., Dlugosz, A. A., Hansen, L. A., Tennenbaum, T., Lichti, U., Yee, D., LaMantia, C., Mourton, T., Herrup, K., Harris, R. C. et al. (1995). Targeted disruption of mouse EGF receptor: effect of genetic background on mutant phenotype. *Science* **269**, 230-234.

Towbin, J. A. and Belmont, J. (2000). Molecular determinants of left and right outflow tract obstruction. *Am. J. Med. Genet.* **97**, 297-303.

Tropepe, V., Sibilia, M., Ciruna, B. G., Rossant, J., Wagner, E. F. and van der Kooy, D. (1999). Distinct neural stem cells proliferate in response to EGF and FGF in the developing mouse telencephalon. *Dev. Biol.* **208**, 166-188.

Vivian, J. L., Gan, L., Olson, E. N. and Klein, W. H. (1999). A hypomorphic myogenin allele reveals distinct myogenin expression levels required for viability, skeletal muscle development, and sternum formation. *Dev. Biol.* **208**, 44-55.

Yarden, Y. (2001). The EGFR family and its ligands in human cancer. signalling mechanisms and therapeutic opportunities. *Eur. J. Cancer Suppl.* **37**, S3-S8.

Yarden, Y. and Sliwkowski, M. X. (2001). Untangling the ErbB signalling network. *Nat. Rev. Mol. Cell Biol.* **2**, 127-137.

Yoon, Y. M., Oh, C. D., Kim, D. Y., Lee, Y. S., Park, J. W., Huh, T. L., Kang, S. S. and Chun, J. S. (2000). Epidermal growth factor negatively regulates chondrogenesis of mesenchymal cells by modulating the protein kinase C-alpha, Erk-1, and p38 MAPK signaling pathways. *J. Biol. Chem.* **275**, 12353-12359.